Synthesis of Copper-Promoted CeO_2 Catalysts

Matías Jobbágy,*,† Fernando Mariño,‡ Betina Schönbrod,‡ Graciela Baronetti,‡ and Miguel Laborde‡

INQUIMAE, Facultad de Ciencias Exactas y Naturales, Universidad de Buenos Aires, Pabellón II, Ciudad Universitaria, C1428EHA - Buenos Aires, Argentina, and Laboratorio de Procesos Catalíticos, Facultad de Ingeniería, Universidad de Buenos Aires, Pabellón de Industrias, Ciudad Universitaria, C1428EHA - Buenos Aires, Argentina

Received November 4, 2005. Revised Manuscript Received February 6, 2006

The urea method is explored for a high-yield preparation of $CuO-CeO_2$ catalysts precursors. Solutions containing urea, $Ce(NO_3)_3$, and $Cu(NO_3)_2$ were aged at 363 K for 5 h, achieving a quantitative coprecipitation in the form of amorphous Cu(II)−Ce(III) basic carbonates, with Cu(II) contents up to 40%. The mixed precursors were characterized by PXRD, SEM, EDS, FTIR, and TG. Upon mild thermal treatment under air atmosphere, i.e., $T = 723$ K, powders were readily converted into CuO-promoted nanometric ceria. No Tenorite (CuO) segregation is observed after annealing at 873 K. The binary oxides were characterized by means of temperature-programmed reduction (TPR) and a test reaction for the preferential oxidation of carbon monoxide (CO-PROX), achieving the best performance with samples containing around 20% in copper atoms.

Introduction

Pure hydrogen is the ideal fuel for proton exchange membrane fuel cells (PEMFC) but the CO content in the H_2 inlet needs to be reduced by means of a preferential oxidation of the former (CO-PROX reaction). The $CuO-CeO_2$ catalysts have demonstrated success to this aim,[1−4] instead of the costly supported noble metal ones.[5−8] In addition, those binary oxides are also useful for catalyzing the SO_2[9] or NO_x[10] reduction as well as phenol's oxidation.[11]

A common procedure to prepare the $CuO-CeO_2$ catalysts consists of the impregnation of CeO_2 particles with Cu(II) moieties,[12] but the Cu(II) ions tend to segregate from CeO_2 supports in the form of nonactive Tenorite (CuO) particles, even for low Cu(II) loadings.[13,14]

An alternative approach is based on the oxidation of Ce−Cu binary precursors into highly interdispersed Cu(II)−Ce(IV) oxides.[15] The synthesis of the mixed Ce(III) and Cu(II) precursors is commonly achieved by heterogeneous coprecipitation in basic media,[16−20] the inhomogeneities during the formation of solids being an inherent vice of this procedure.[21]

As an improvement in the latter, the urea method provides an alternative highly reproducible homogeneous precipitation process, which makes use of the thermal hydrolysis of urea into ammonium carbonate.[22] Several binary precursors of Cu(II)-containing lanthanide oxides were obtained with this method.[23,24]

Despite Ce(III/IV)−Cu(II) solids being obtained using this method in the past,[25,26] essential aspects concerning the formation of the mixed precursors as well as their thermal transformation to the mixed oxides require a deeper exploration.[27] The aim of this work is to evaluate the possibilities and limitations of the urea method, in the synthesis of mixed

* Corresponding author. E-mail: jobbag@qi.fcen.uba.ar.
† INQUIMAE, Facultad de Ciencias Exactas y Naturales
‡ Laboratorio de Procesos Catalíticos, Facultad de Ingeniería

(1) Kim, D.; Cha, J. *Catal. Lett.* **2003**, *86*, 107.
(2) Wang, J.; Tsai, D.; Huang, T. *J. Catal.* **2002**, *208*, 370.
(3) Kandoi, S.; Gokhale, A.; Grabow, L.; Dumesic, J.; Mavrikakis, M. *Catal. Lett.* **2004**, *93*, 93.
(4) Xiaoyuan, J.; Guanglie, L.; Renxian, Z.; Jianxin, M.; Yu, C.; Xiaoming, Z. *Appl. Surf. Sci.* **2001**, *173*, 208.
(5) Oh, S.; Sinkevitch, R. *J. Catal.* **1993**, *142*, 254.
(6) Mariño, F.; Descorme, C.; Duprez, D., *Appl. Catal. B* **2004**, *54*, 59.
(7) Haruta, M. *Catal. Today* **1997**, *36*, 153.
(8) Schubert, M.; Venugopal, A.; Kahlich, M.; Plzak, V.; Behm, R. *J. Catal.* **2004**, *222*, 32.
(9) Liu, W.; Wadia, C.; Flytzani-Stephanopoulos, M. *Catal. Today* **1996**, *28*, 391.
(10) Bera, P.; Aruna, S. T.; Patil, K. C.; Hegde, M. S. *J. Catal.* **1999**, *186*, 36.
(11) Hočevar, S.; Krasovec, U. O.; Orel, B.; Arico, A. S.; Kim, H. *Appl. Catal. B* **2000**, *28*, 113.
(12) Hu, Y.; Dong, L.; Wang, J.; Ding, W.; Chen, Y. *J. Mol. Catal.* **2000**, *162*, 307.
(13) Luo, M. F.; Zhong, Y. J.; Yuan, X. X.; Zheng, X. M. *Appl. Catal. A* **1997**, *162*, 121.
(14) Xiaoyuan, J.; Liping, L.; Yingxu, C.; Xiaoming, Z. *J. Mol. Catal. A* **2003**, *197*, 193.
(15) Skårman, B.; Nakayama, T.; Grandjean, D.; Benfield, R. E.; Olsson, E.; Niihara, K.; Wallenberg, L. R. *Chem. Mater.* **2002**, *14*, 3686.
(16) Zimmer, P.; Tschöpe, A.; Birringer, R. *J. Catal.* **2002**, *205*, 339.
(17) Shen, W. J.; Ichihashi, Y.; Matsumura, Y. *Catal. Lett.* **2002**, *83*, 33.
(18) Lamonier, C.; Bennani, A.; D'Huysser, A.; Aboukaïs, A.; Wrobel, G. *J. Chem. Soc., Faraday Trans.* **1996**, *92* (*1*), 131.
(19) Liu, Y.; Hayakawa, T.; Susuki, K.; Hamakawa, S.; Tsunoda, T.; Ishii, T.; Kumagi, M. *Appl. Catal. A* **2002**, *223*, 137.
(20) Hočevar, S.; Batista, J.; Levec, J. *J. Catal.* **1999**, *184*, 39.
(21) Harrison, P. G.; Ball, I. K.; Azalee, W.; Daniell, W.; Goldfarb, D. *Chem. Mater.* **2000**, *12*, 3715.
(22) Soler Illia, G. J. A. A.; Jobbágy, M.; Candal, R. J.; Regazzoni; A. E.; Blesa, M. A. *J. Dispersion Sci. Technol.* **1998**, *19*, 207.
(23) Candal, R. J.; Regazzoni, A. E.; Blesa, M. A. *Colloids. Surf. A* **1993**, *79*, 191.
(24) Ribot, F.; Kratohvil, S.; Matijević, E. *J. Mater. Res.* **1989**, *4*, 1123.
(25) Kundakovic, L.; Flytzani-Stephanopoulos, M. *Appl. Catal. A* **1998**, *171*, 13.
(26) Li, Y.; Fu, Q.; Flytzani-Stephanopoulos, M. *Appl. Catal. B* **2000**, *27*, 179.
(27) Liu, W.; Fu, Q.; Stephanopoulos, M. F. *Catal. Today* **2004**, *93*, 241.

10.1021/cm052437h CCC: $33.50
Published on Web 03/08/2006

Cu(II)−Ce(III) particles, as precursors for copper-promoted−CeO_2 catalysts. A discussion concerning the (co)-precipitation process of Cu(II) and Ce(III) ions is offered. Textural, chemical, and structural characteristics of the binary precursors and their corresponding Cu(II)−Ce(IV) oxides is presented, in addition to the thermal evolution of the former into the latter. The reducibility of the Cu(II) moieties as well as Ce(IV) ones is contrasted with the catalytic performance in the CO-PROX reaction.

Experimental Section

Synthesis and Characterization of Precursors. Stock solutions of Ce(III) nitrate and Cu(II) nitrate (0.5 and 0.1 mol dm^{-3}, respectively) were prepared by dissolving $Ce(NO_3)_3 \cdot 6H_2O$ and $Cu(NO_3)_2 \cdot 3H_2O$ in water, respectively, filtered through 0.2 μm pore-size cellulose nitrate membranes, and stored in plastic bottles. All solutions were made up using analytical-grade reagents and deionized water (18 MΩ-cm) obtained from a Milli-Q apparatus. Precursors were prepared by aging mixed cerium(III)−copper(II) urea containing solutions at 363.0 ± 0.5 K for different periods. In all cases, the concentrations of urea and total metal (i.e., $[Ce(III)]_o + [Cu(II)]_o$) were kept constant at 0.5 mol dm^{-3} and 5.0×10^{-2} mol dm^{-3}, respectively. The ratio of Cu(II) to total metal, $X = [Cu(II)]_o/([Ce(III)]_o + [Cu(II)]_o) \times 100$, was varied between 0 and 60. In the following, the samples will be named CeCuX, where X is the nominal percentage of Cu(II). Typically, precipitation experiments were performed as follows: starting solutions were prepared by mixing the necessary amounts of the stock solutions, solid urea, and water to yield the desired reactant concentrations. Then 100 cm^3 of filtered aliquots were poured into 150 cm^3 screw-capped plastic bottles, which were then placed in a thermostated water bath preheated at the working temperature. After pre-fixed time intervals, the bottles were removed and immersed in an ice-water bath to quench the reaction. Precipitated solids were collected by filtration through 0.2 μm pore-size cellulose nitrate membranes, washed three times with cold water, and dried at 343 K overnight. Supernatant solutions were stored for chemical analyses; pH was measured (±0.02 units) using a combined glass electrode, and Cu(II) and Ce(III) concentrations were determined, within 1%, by atomic absorption spectrometry.

Mixed oxides were synthesized by heating precursors under an air flow of 50 cm^3 min^{-1} from room temperature to 723 and 873 K (holding the final temperature for 30 min) in a thermogravimetric Shimadzu TG 51 apparatus, using a 3.0 K min^{-1} temperature ramp.

All synthesized solids were characterized by powder X-ray diffraction (PXRD) using the graphite-filtered Cu Kα radiation (λ = 1.5406 Å), scanning electron microscopy (SEM), energy-dispersive X-ray spectroscopy (EDS), and Fourier transform infrared spectroscopy (FTIR). Crystal size was estimated using Scherrer's equation.

Temperature-Programmed Reduction (TPR). TPR experiments were performed with a thermal conductivity detector, on samples of 30 mg in a 98% (molar) nitrogen and 2% (molar) hydrogen gas mixture, using a gas flow rate of 100 mL min^{-1} and a temperature range of 293−1123 K with a temperature ramp rate of 5 K/min. Prior to TPR tests the samples were treated at 723 K for 1 h under air flow (ramp rate: 10 K min^{-1}; flow 100 mL min^{-1}) to clean the surface.

Catalytic Evaluation. For all samples, catalytic performance was evaluated in a fixed-bed glass reactor using 200 mg of catalyst and a total inlet flow of 230 mL min^{-1}, with a 89.5% H_2, 2.3% CO, 1.7% O_2 (λ = 1.5), N_2 balance (6.5%) composition. The catalytic performance was evaluated at several temperatures in the range 373−523 K. Reported values of conversions and selectivity correspond to steady-state values.

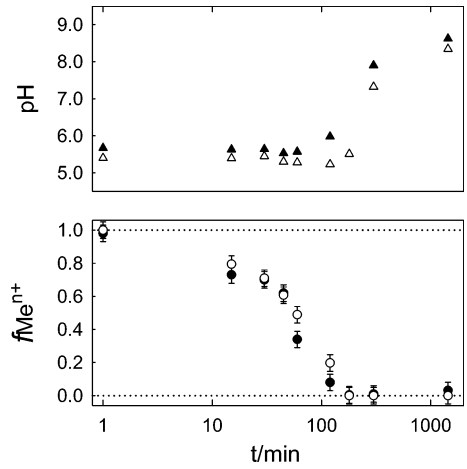

Figure 1. (Upper panel) Evolution pH as a function of aging time at 363 K for the single sample CeCu0 (△) and the binary sample CeCu10 (▲); initial solution composition: $[Me]_0 = 0.05$ M; $[urea]_0 = 0.5$ M. (Lower panel) Fraction of Cu(II) (●) and Ce(III) (○) remaining in solution as a function of aging time at 363 K for the binary sample CeCu10.

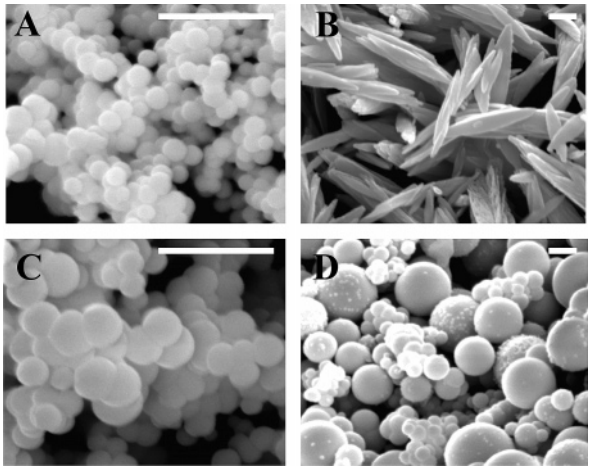

Figure 2. SEM micrographs of sample CeCu0 aged at 363 K for 1 h (A) and 5 h (B); sample CeCu10 aged at 363 K for 1 h (C) and 5 h (D). Scale bar = 1 μm.

Results and Discussion

Precipitation of Precursors. Figure 1A shows the evolution of pH for the CeCu0 and CeCu10 samples, during the aging at 363 K. In both cases, during the first 2 h, the precipitation process consumes the base released by the decomposition of urea, fixing the pH value close to 5.40 in the case of the CeCu0 system and 5.60 for the CeCu10 one. After 5 h, the precipitation is complete and pH turns alkaline. Chemical analysis of the CeCu10 solution during the aging revealed that the fractions of Cu(II) and Ce(III) remaining in the mother liquors are identical (Figure 1B), indicating the coprecipitation of both cations.

SEM observation of the CeCu0 and CeCu10 samples aged at different times (Figure 2) revealed noticeable differences. After 1 h of aging, the CeCu0 samples consisted of monodispersed spherical particles of 0.2 μm; after 5 h of aging the solid evolved into 4 ± 1 μm long ellipsoids.[28] In

(28) Matijević, E.; Hsu, W. P. *J. Colloid Interface Sci.* **1987**, *118*, 506.

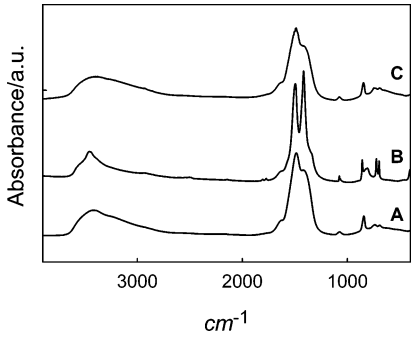

Figure 3. FTIR spectra of sample CeCu0 aged at 363 K for 1 h (A) and 5 h (B) and sample CeCu10 aged at 363 K for 5 h (C), recorded on KBr disks.

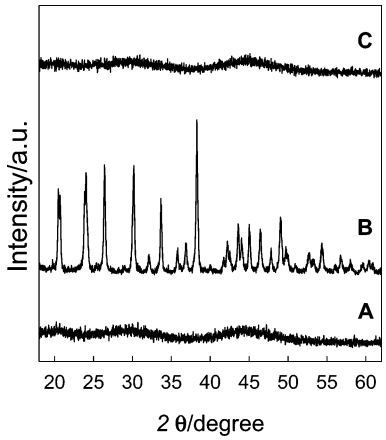

Figure 4. PXRD patterns of sample CeCu0 aged at 363 K for 1 h (A) and 5 h (B) and sample CeCu10 aged at 363 K for 5 h (C).

the case of the CeCu10 sample, after 1 h of aging, polydispersed spherical particles of 0.3 ± 0.1 μm are present. After 5 h of aging, the polydispersion increases, with particles ranging from 0.2 to 2 μm; interestingly, the transformation into ellipsoid-like particles do not take place. In accordance with solution analysis, EDS probe revealed that the Cu/Ce ratio remained constant as a function of aging time. These results are highly reproducible; however, other shapes have been observed when the urea to Ce(III) ratio and/or temperature were different than the ones applied in our study.[28]

For all samples, FTIR spectra are typical of a metallic hydrated carbonate (see Figure 3).[29] The bands centered at 1500, 1400, 1090, 850, 730, and 680 cm^{-1} correspond to the $\nu(OCO_2)$, $\nu(CO_3)$, $\nu(C{=}O)$, $\delta(CO_3)$, $\delta(OCO)$, and $\rho(OCO)$ modes, respectively, of carbonate ions in the C_{2v} symmetry. The broad band that ranges from 3000 to 3500 cm^{-1} corresponds to the OH stretching, with a contribution of carbonate interacting with water. The peak centered at 1630 cm^{-1} can be ascribed to the H_2O bending mode. The sharper bands observed for the CeCu0 after 5 h of aging reveals a higher structural order.

Figure 4 presents the PXRD patterns of samples CeCu0 and CeCu10, obtained after different aging times at 363 K. The single Ce(III) sample, aged for 1 h, presents two extremely broad reflections centered at 30° and 45°, characteristic of an ill-crystallized Ce(III) ammonium carbonate hydrate, as reported by Li et al.[30] After 5 h of aging, this sample evolves into well-crystallized $Ce_2O(CO_3)_2{\cdot}H_2O$,[31] whereas the mixed sample preserves its quasi-amorphous nature.

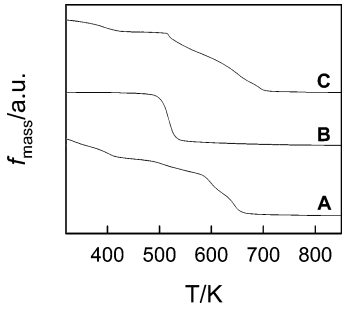

Figure 5. TG curves of sample CeCu0 aged at 363 K for 1 h (A) and 5 h (B); sample CeCu10 aged at 363 K for 5 h (C), decomposed in air (20 mL min^{-1}) at 3 K min^{-1}.

Figure 5 shows the TG traces of samples CeCu0−10 decomposed in air. For the CeCu0 sample aged for 5 h, the thermal decomposition proceeds in a single step centered at 517 K, in accordance with eq 1.[32,33]

$$^1/_2O_2 + Ce_2O(CO_3)_2{\cdot}H_2O \rightarrow 2CeO_2 + 2CO_2 + H_2O \quad (1)$$

The TG trace of the CeCu10 sample aged for 5 h is more complex; below 420 K a mass loss associated with the departure of weakly adsorbed water can be observed. Close to 520 K the massive decomposition starts, but in a less defined way, exhibiting two main steps centered around 550 K and 650 K. Previous reports indicate that those steps correspond to the departure of ammonium and a fraction of carbonate anions followed by the final decarboxylation, respectively.[30] This behavior is common to many amorphous lanthanide-doped Ce(III) basic ammonium carbonates.[34−37] Similar behavior was observed for the CeCu0 sample aged for 1 h, in accordance with SEM inspection and FTIR data.

Regarding the precipitation of the mixed CeCu10 particles, a tentative mechanism can be suggested, taking into account the behavior of the single systems. The Ce(III) system precipitates in the form of amorphous hydrated carbonate particles of spherical shape, at a pH value around 5.40. Only after aging, those particles evolve to more stable crystalline $Ce_2O(CO_3)_2{\cdot}H_2O$ ellipsoids. Such transformation is difficult to explain in terms of ordered aggregation since TG also indicates changes in chemical composition. Dissolution and reprecipitation being the most plausible pathway, in accordance with the Ostwald step rule.[38,39] For the case of single Cu(II) system, it was reported that once the solution reaches

(29) Klissurski, D. G.; Uzunova, E. L. *Chem. Mater.* **1991**, *3*, 1060.
(30) Li, J. G.; Ikegami, T.; Mori, T.; Wada, T. *Chem. Mater.* **2001**, *13*, 2913.
(31) Wang, H.-C.; Lu, C.-H. *Mater. Res. Bull.* **2002**, *37*, 783.
(32) Lu, C. H.; Wang, H. C. *Mater. Sci. Eng B* **2002**, *90*, 138.
(33) Padeste, C.; Cant, N. W.; Trimm, D. L. *Catal. Lett.* **1994**, *24*, 95.
(34) Tok, A. I. Y.; Luo, L. H.; Boey, F. Y. C. *Mater. Sci. Eng. A* **2004**, *383*, 229.
(35) Colón, G.; Navío, J. A.; Monaci, R.; Ferino, I. *Phys. Chem. Chem. Phys.* **2000**, *2*, 4453.
(36) Aiken, B.; Hsu, W. P.; Matijevic, E. *J. Am. Ceram. Soc.* **1988**, *71*, 845.
(37) Li, J. G.; Ikegami, T.; Wang, Y.; Mori, T. *J. Am. Ceram. Soc.* **2003**, *86*, 915.
(38) Ostwald, W. *Z. Phys. Chem.* **1897**, *22*, 289.
(39) Soler Illia, G. J. A. A.; Jobbágy, M.; Regazzoni, A. E.; Blesa, M., *Chem. Mater.* **1998**, *11*, 3140.

a critical oversaturation condition with respect to $Cu(OH)_2$, this phase precipitates in the form of amorphous spherical particles, at a pH value around 6.20.[40] The aging allows the dissolution and reprecipitation into different crystalline Cu(II) basic salts, depending on the counteranion present in solution.[41,42] For both cations, the spherical shape in addition to the amorphous nature of particles that first precipitate suggests that the homogeneous precipitation proceeds with the formation of primary nanometric amorphous units (singlets) which aggregate into secondary micrometric spherical ones, as was documented by Matijević et al.[43,44] In the case of the mixed sample CeCu10, the Cu(II) ions coprecipitate with Ce(III) at a pH value around 5.60, just in the solubility limit of $Cu(OH)_2$. Probably, the new born Ce(III) primary particles allow the precipitation of Cu(II) ions, before reaching the critical supersaturation with respect to $Cu(OH)_2$, due to the sorption of hydroxylated Cu(II) polymeric moieties and/or due to a surface precipitation process of Cu(II) ions onto Ce(III) singlets.[45] Then, the resulting Cu(II)-loaded Ce(III) singlets aggregate into the mixed amorphous secondary particles, observed by SEM. In the explored conditions, those binary precursors are hindered from segregating into the pure crystalline basic carbonates (stable phases), preserving not only the original shape but also the desired high degree of interdispersion.

Limit of Segregation. To establish the composition limits in which the coprecipitation mechanism operates, the Cu(II) content was gradually increased up to 60%. All the samples exhibit a similar main component of an amorphous PXRD pattern, identical to that of the CeCu10 sample. In addition, the samples CeCu50−60 exhibit a sharp peak centered at 25.7°, which corresponds to the (002) reflection of lamellar $Cu_2NO_3(OH)_3$ (see Supporting Information).[46] The preponderance of $Cu_2NO_3(OH)_3$ over the typical $Cu_2CO_3(OH)_2$ obeys to the high nitrate concentration employed in the present case.[47]

SEM-EDS inspection revealed that CeCu20−60 samples are constituted of polydispersed spherical particles. For each sample, a constant Cu/Ce ratio was found in the different particles, irrespective of their size. Meanwhile, in samples CeCu50−60, the amorphous mixed spheres coexist with a minor fraction of large crystalline ones (see Supporting Information), in which not even traces of Ce atoms were present. The maximum Cu content observed in the amorphous spherical particles is ca. 45% for both samples. All the mixed samples up to 40% in Cu(II) ions presented similar thermal decomposition behavior (see Supporting Information).

Figure 6 shows the PXRD of the samples decomposed in air at 723 K; CeO_2 (cerianite) is present in all cases,

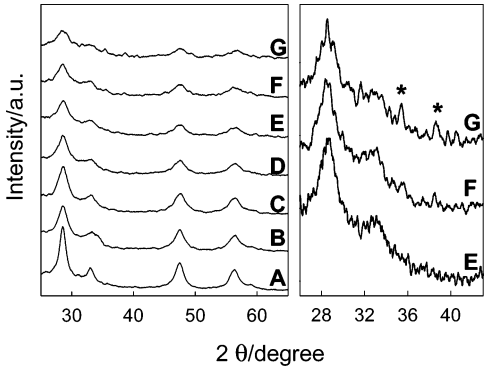

Figure 6. PXRD patterns of samples CeCu0 (A), CeCu10 (B), CeCu20 (C), CeCu30 (D), CeCu40 (E), CeCu50 (F), and CeCu60 (G) decomposed in air (20 mL min^{-1}) at 3 K min^{-1}, holding a final temperature of 723 K for 30 min. On the expanded pattern (right), asterisks denote the presence of Tenorite (CuO).

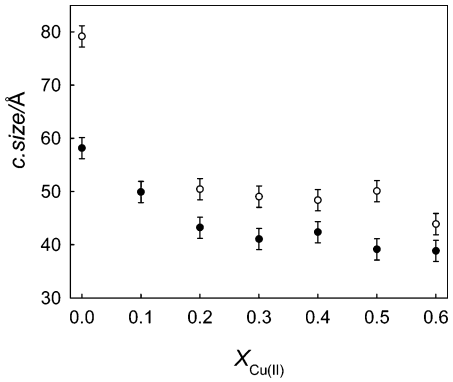

Figure 7. Influence of Cu(II) content in the crystal size of cerianite (CeO_2) in the (220) (●) and (111) (○) directions. All samples where decomposed in air (20 mL min^{-1}) at 3 K min^{-1}, holding the final temperature of 723 K for 30 min.

confirming the oxidation of Ce(III) to Ce(IV). However, the wide peaks and even certain asymmetries tell about the low degree of crystallization of the obtained oxides. Samples CeCu60 and CeCu50 (in a minor way) also show traces of Tenorite (CuO), as can be expected for precursors in which Cu(II) basic nitrate is present. As was pointed out in the preceding section, the Cu(II) is well-dispersed within the precursors of up to 40% and this condition prevents the segregation of crystalline CuO. It is known that CeO_2 constitutes stable solid solution up to 20% with many cations,[48] including Cu(II)[11,49] however, the ill-crystallized oxides obtained in the present case make impossible the quantification of any displacement in the cell parameter of cerianite. Figure 7 shows the effect of Cu(II) content in the crystalline size of CeO_2 along (220) and (111) directions, showing that the presence of Cu(II) ions hinders the crystalline growth of cerianite, as was reported previously.[50] For pure CeO_2, discrepancies in the crystalline size can be originated in the characteristic strain of these nanoparticles;[51] even the inclusion of Cu ions in the lattice can also contribute to this effect.[50] All the samples reflect a slight crystal growth

(40) Soler Illia, G. J. A. A. Ph.D. Thesis, Universidad de Buenos Aires, 1998.
(41) Candal, R. J.; Regazzoni, A. E.; Blesa, M. A. *J. Mater. Chem.* **1992**, *2*, 657.
(42) Soler Illia, G. J. A. A.; Candal, R. J.; Regazzoni, A. E.; Blesa, M., *Chem. Mater.* **1997**, *9*, 184.
(43) Privman, V.; Goia, D. V.; Park, J.; Matijeviæ, E. *J. Colloid Interface Sci.* **1999**, *213*, 36.
(44) Park, J.; Privman, V.; Matijeviæ, E. *J. Phys. Chem. B* **2001**, *105*, 11630.
(45) Towle, S. N.; Bargar, J. R.; Brown, G. E.; Parks, G. A. *J. Colloid Interface Sci.* **1997**, *187*, 62.
(46) Meyn, M.; Beneke, K.; Lagaly, G. *Inorg. Chem.* **1993**, *32*, 1209.
(47) Candal, R. J. Ph.D. Thesis, Universidad de Buenos Aires, 1995.
(48) Huang, W.; Shuk, P.; Greenblatt, M. *Chem. Mater.* **1997**, *9*, 2240.
(49) Gayen, A.; Priolkar, K. R.; Shulka A. K.; Ravishankar, N.; Hegde, M. S. *Mater. Res. Bull.* **2005**, *40*, 421.
(50) Wang, X.; Rodriguez, J. A.;Hanson, J. C.; Gamarra, D.; Martínez-Arias, A.; Fernández-García, M. *J. Phys. Chem. B* **2005**, *109*, 19595.
(51) Zhou, X.-D.; Heubner, W. *Appl. Phys. Lett.* **2001**, *79*, 3512.

Table 1. Comparison of Several Methods for the Synthesis of Mixed Cu(II)−Ce(IV) Oxides

method	reagents and synthesis conditions	A_T	(Cu,Ce)Ox	T_S	S_A (BET)	Ref.
CB	$Cu(NO_3)_2/(NH_4)_2Ce(NO_3)_6$-carboazide		0−40%	60%	40-60 m^2/g	58
CB	$Cu(NO_3)_2/Ce(NO_3)_3$-citric acid	923 K	0−20%	30%	17-35 m^2/g	59
CB	$Cu(NO_3)_2/Ce(NO_3)_3$-citric acid	823 K	0−15%	25%	40-78 m^2/g	60
IGC	Cu/Ce alloy + 1 Torr O_2, 298 K		0−29%	54%	55-60 m^2/g	15
CP	$Cu(NO_3)_2/Ce(NO_3)_3$-NaOH- 333 K	673 K	0−16%	33%	28-97 m^2/g	18
CP	$Cu(NO_3)_2/Ce(NO_3)_3$-NaOH-363 K	723 K	0−10%	20%	96 m^2/g	19
CP	$Cu(NO_3)_2/Ce(NO_3)_3$-Na_2CO_3-298 K	773 K	0−05%	10%	22-28 m^2/g	20
ME	$Cu(NO_3)_2/Ce(NO_3)_3$-heptane-TritonX100-TMAH	773 K	0−20%		130-151 m^2/g	50
HP	$Cu(NO_3)_2/(NH_4)_2Ce(NO_3)_6$/10%$La^{III}$-Urea-373 K	923 K	0−15%	40%	46-92 m^2/g	26
HP	$Cu(NO_3)_2/Ce(NO_3)_3$-urea-363 K	723 K	0−40%	50%	25-90 m^2/g	*

HP: Homogeneous Precipitation; **CP**: Coprecipitation; **IGC**: Inert Gas Condensation; **CB**: Combustion method; **ME**: Microemulsion method; $\mathbf{A_T}$: Annealing temperature; **(Cu,Ce)Ox:** Range in which copper appears apparently dissolved in the fluorite structure; i.e., no Tenorite (CuO) segregation is detected on the basis of PXRD; $\mathbf{S_A}$: Surface area; $\mathbf{T_S}$: Tenorite (CuO) segregation observed by PXRD; * This work.

when the annealing temperature increases to 873 K, though no Tenorite segregation is observed for samples with Cu(II) contents of 40% or lower (see Supporting Information).[52,53]

Table 1 presents data of the mixed oxides obtained by the typical procedures available in the literature; those oxides are currently characterized by PXRD since the appearance of tenorite's peaks (T_S composition) demonstrates CuO segregation. Although this technique is silent to the incipient segregation, in the form of small or amorphous CuO clusters, the range of compositions in which no Tenorite's segregation is observed (range of dispersion, $CuO{\cdot}CeO_2$) was chosen as a criterium of the degree of interdispersion achieved by each procedure. In contrast with the other coprecipitation procedures, the present low-temperature method extends this range, preserving high yields and reaching interdispersion degrees that only high-temperature procedures, like the combustion method, had offered before.[54−60]

Temperature-Programmed Reduction of the Mixed Oxides. The H_2-TPR profiles of the oxides with increasing copper content are shown in Figure 8, in the temperature range 323−1173 K. The low-temperature reduction region, commonly associated with Cu(II) centers and normalized with respect to the total copper content of each sample, is shown with more detail in Figure 8A. Under our experimental conditions, the reduction of pure CuO gives a single peak centered at 515 K while the reduction profiles of all samples reflect a quantitative H_2 consumption taking place at a lower temperature (between 398 and 498 K), demonstrating that Cu(II) is dispersed enough in the ceria matrix to enhance its reducibility. The reduction profile is complex: three overlapped reduction peaks, named as α, β, and γ (ordered by increasing temperature), indicate that at least three kinds of copper species are present.[54,61] It should be noted that not only the position but also the relative intensity

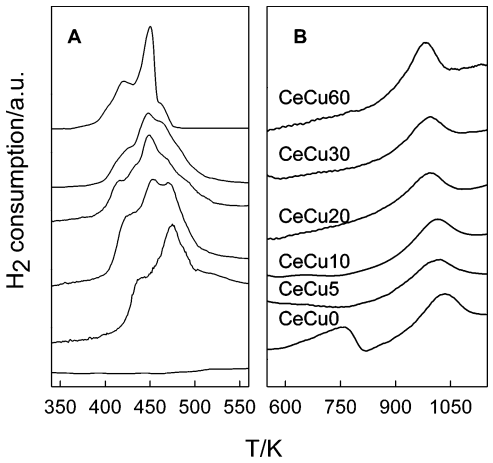

Figure 8. Temperature-programmed reduction trace (expressed as H_2 consumption, in arbitrary units) of samples with increasing copper content. The 350−550 K range (A) is normalized with respect to the atomic copper content of each sample while the 580−1125 K range (B) is normalized to the cerium one.

of these three peaks change with the copper content of the catalyst. Figure 8B shows the high-temperature TPR trace normalized with respect to the cerium content of each sample. The nano-ceria obtained from sample CeCu0 shows two wide peaks centered at 763 and 1043 K, associated with the surface capping oxygen and bulk oxygen atoms, respectively.[62] Interestingly, the first peak (763 K) is absent for all the binary samples while the high-temperature peak (1043 K) shifts to lower temperatures as the copper content increases, across the studied range of compositions. Then, the presence of copper, even with contents of 5 %, affects not only the surface redox properties of the cerianite but also the bulk ones. The redox properties of both cations are mutually affected by the presence of each other, and their sequential reduction cannot be seen as independent processes, as was demonstrated by Martinez-Arias et al.[63,64]

Catalytic Performance. The success of preferential oxidation of CO (CO-PROX reaction) is conditioned by the competition between the desired oxidation of carbon mon-

(52) Fernández-García, M.; Martínez-Arias, A.; Hanson, J. C.; Rodriguez, J. A. *Chem. Rev.* **2004**, *104*, 4063.
(53) Chen, P. L.; Chen, I. W. *J. Am. Ceram. Soc.* **1996**, *79*, 3129.
(54) Avgouropoulos, G.; Ioannides, T. *Appl. Catal. A* **2003**, *244*, 155.
(55) Bera, P.; Priolkar, K. R.; Sarode, P. R.; Hegde, M. S.; Emura, S.; Kumashiro, R.; Lalla, N. P. *Chem. Mater.* **2002**, *14*, 3591.
(56) Avgouropoulos, G.; Ioannides, T.; Matralis, H. *Appl. Catal. B* **2005**, *56*, 87.
(57) Papavasiliou, J.; Avgouropoulos, G.; Ioannides, T. *Catal. Commun.* **2004**, *5*, 231.
(58) Rao, G. R.; Sahu, H. R.; Mishra, B. G. *Colloids Surf. A* **2003**, *220*, 261.
(59) Shan, W.; Shen, W.; Li, C. *Chem. Mater.* **2003**, *15*, 4761.
(60) Marbán, G.; Fuertes, A. B. *Appl. Catal. B* **2005**, *57*, 43.
(61) Tschöpe, A.; Markmann, J.; Zimmer, P.; Birringer, R.; Chandwick, A. V. *Chem. Mater.* **2005**, *17*, 3935.
(62) Giordano, F.; Trovarelli, A.; de Leitenburg, C.; Giona, M. *J. Catal.* **2000**, *193*, 273.
(63) Martínez-Arias, A.; Hungría, A. B.; Fernández-García, M.; Conesa, J. C.; Munuera, G. *J. Phys. Chem. B* **2004**, *108*, 17983.
(64) Wang, X.; Rodriguez, J. A.; Hanson, J. C.; Gamarra, D.; Martínez-Arias, A.; Fernández-García, M. *J. Phys. Chem. B* **2006**, *110*, 428.

Table 2. Characteristics of the CeCuX Samples an Their Catalytic Performance[a]

sample	precursor	723 K	S_A (BET)	CO_{conv}	selectivity[b]	T_{max}
CeCu5	*am*-BC	C		76 ± 2%	51 ± 2%	503 ± 5 K
CeCu10	*am*-BC	C	21 ± 2 m^2/g	98 ± 2%	63 ± 2%	471 ± 5 K
CeCu20	*am*-BC	C	22 ± 2 m^2/g	98 ± 2%	63 ± 2%	463 ± 5 K
CeCu30	*am*-BC	C	28 ± 2 m^2/g	87 ± 2%	55 ± 2%	429 ± 5 K
CeCu60	*am*-BC + BN	C + T	51 ± 3 m^2/g	70 ± 2%	47 ± 2%	432 ± 5 K

[a] *am*: amorphous; C: cerianite, CeO_2; OCH: oxicarbonatehydrate, $Ce_2O(CO_3)_2 \cdot H_2O$; BC: basic carbonate; BN: basic nitrate, $Cu_2NO_3(OH)_3$; T: Tenorite, CuO; CO_{conv}: maximum percentage of CO conversion; T_{max}: temperature of maximum CO conversion. [b] Observed at maximum percentage of CO conversion.

oxide and other undesired side reactions (CO and CO_2 methanation, oxidation of H_2, and coke formation). For all catalytic determinations, not even traces of methane were detected at the reactor outlet, so both methanations can be ruled out. Moreover, carbon balance showed that the CO_2 production is in good agreement with the CO consumption, so coking over such catalysts could also be disregarded. For all samples, a maximum value for CO conversion was observed, before hydrogen oxidation began to compete. It is accepted that the Ce(III)/Ce(IV) redox couple of the fluorite-type CeO_2 allows the reversible uptake of oxygen, while CO (and H_2) uses mostly copper atoms as the adsorption sites.[65,66]

Table 2 shows a general trend in which the optimal temperature decreases as the copper content of the sample increases, indicating that the undesired hydrogen oxidation reaction proceeds at lower temperatures on the samples of higher copper content. In the present case, the best conversions and selectivities where found for the samples with copper atomic contents equal to 10 and 20%, with the maximum performance achieved at a lower temperature, for the latter sample. At 463 K, a CO conversion higher than 98% and a CO_2 selectivity equal to 63% were achieved. A higher copper content allow good CO conversion at lower temperatures, in detriment of the selectivity and the maximum CO conversion.

Conclusions

The urea method presented in this work has allowed us to prepare in a simple and reproducible way mixed Cu(II)−Ce(III) basic carbonates in a wide range of compositions. Those precursors, after moderate thermal treatment, evolve into Cu(II)-promoted nanoceria catalysts that prevent Tenorite segregation even with copper contents as high as 40%. The catalysts reported in this work are comparable to other catalysts reported in the literature, even if the conditions used in the present work are less favorable (lower contact times and lower oxygen excess). The catalytic activity is optimal for the CeCu20 sample.

Acknowledgment. This work was supported by grants from ANPCYT and Universidad de Buenos Aires. G.B., M.J., M.L., and F.M. are members of CONICET. The authors are indebted to Prof. M. A. Blesa (UAQ-CNEA) for the use of the SEM-EDS facility and to Mr. R. Tejeda for his technical assistance. We are indebted to Dr. P. Tartaj for helpful discussions. We deeply appreciate the dedication of referees for enhancing the quality of this work.

Supporting Information Available: Five additional figures. This material is available free of charge via the Internet at http://pubs.acs.org.

CM052437H

(65) Liu, W.; Flytzani-Stephanopoulos, M. *J. Catal*. **1995**, *153*, 304.
(66) Sedmak, G.; Hoèevar, S.; Levec, J. *J. Catal.* **2003**, *213*, 135.